Advanced Synthesis & Catalysis

WILEY-VCH

ADVANCED SYNTHESIS & CATALYSIS

RESEARCH ARTICLE OPEN ACCESS

Electrochemical Trifluoromethylchlorosulfonylation of Alkenes via Copper-Mediated SO_2Cl Radical Transfer

Sachini Rodrigo[1] | Melanie S. Sanford[2] | Long Luo[1]

[1]Department of Chemistry, University of Utah, Salt Lake City, Utah, USA | [2]Department of Chemistry, University of Michigan, Ann Arbor, Michigan, USA

Correspondence: Melanie S. Sanford (mssanfor@umich.edu) | Long Luo (long.luo@utah.edu)

Received: 26 August 2025 | **Revised:** 10 August 2025 | **Accepted:** 13 October 2025

Funding: NSF Center for Synthetic Organic Electrochemistry, Grant/Award Numbers: CHE-2002158 CHE-2503773; University of Utah; the Alfred P. Sloan Foundation, Grant/Award Number: FH-2023–20829

Keywords: chlorosulfonyl radical transfer | Cu catalysis | difunctionalization of alkene | electrosynthesis | trifluoromethylchlorosulfonylation

ABSTRACT

This article describes an electrosynthetic method for vicinal trifluoromethylchlorosulfonylation of alkenes using the readily available copper salt $[Cu(MeCN)_4]PF_6$ and triethylamine, without the need for elaborate ligands. This protocol enables efficient and selective addition of CF_3 and SO_2Cl groups across a wide range of unactivated alkenes with broad functional group tolerance, including pyrrole, furan, thiophene, thioethyl, and silyl substituents. The sulfonyl chloride products can be readily transformed into sulfonamides, sulfonates, sulfonyl fluorides, and thiosulfonates. Mechanistic studies provide evidence in support of an electrochemically driven, Cu-mediated SO_2Cl radical transfer mechanism.

1 | Introduction

Vicinal difunctionalization of alkenes represents a powerful and atom-economical approach in modern organic synthesis, enabling the simultaneous addition of two functional groups across a carbon–carbon double bond. This strategy offers an efficient means of building molecular complexity from simple olefins and has found widespread utility in the synthesis of pharmaceuticals, agrochemicals, and complex natural products [1–13].

Among functional groups of high synthetic and biological relevance, the trifluoromethyl (—CF_3) and sulfonyl (—SO_2—) motifs stand out for their unique properties. The CF_3 group plays a critical role in medicinal chemistry as it can enhance the metabolic stability, lipophilicity, and bioavailability of drug candidates [14–17]. Meanwhile, sulfonyl-containing groups, including sulfones, sulfonamides, sulfonates, and sulfonyl fluorides [18], are prevalent in bioactive molecules and also serve as versatile intermediates in organic synthesis (Figure 1a) [19–24]. The derivatization of sulfonyl chlorides (—SO_2Cl) is one of the most convenient methods for accessing sulfonyl-containing functional groups [25]. However, despite their individual importance, the direct and selective installation of both CF_3 and SO_2Cl groups onto alkenes in a single transformation remains a synthetic challenge. This difficulty arises from the inherent instability of sulfonyl chloride precursors and their tendency toward uncontrolled reactivity. In this context, trifluoromethanesulfonyl chloride (CF_3SO_2Cl) [26] has emerged as an attractive bifunctional reagent capable of supplying both CF_3 and SO_2Cl radicals. This dual reactivity presents opportunities for achieving radical-mediated alkene difunctionalization in a single, operationally simple step.

In 2015, Reiser and coworkers reported a photochemical trifluoromethylchlorosulfonylation of alkenes using a $[Cu(dap)_2]Cl$ (dap = 2,9-bis(*para*-anisyl)-1,10-phenanthroline) as catalyst [27]. They proposed a novel dual mechanistic role for the $[Cu(dap)_2]Cl$, wherein the Cu complex acts as both a photocatalyst for CF_3SO_2Cl reduction and as a Cu center that actively participates in C—S bond formation (Figure 1b). Photoexcited Cu(I) complex $[Cu(dap)_2]Cl^*$ undergoes single-electron transfer to reduce CF_3SO_2Cl, generating a CF_3 radical and a Cu-SO_2Cl

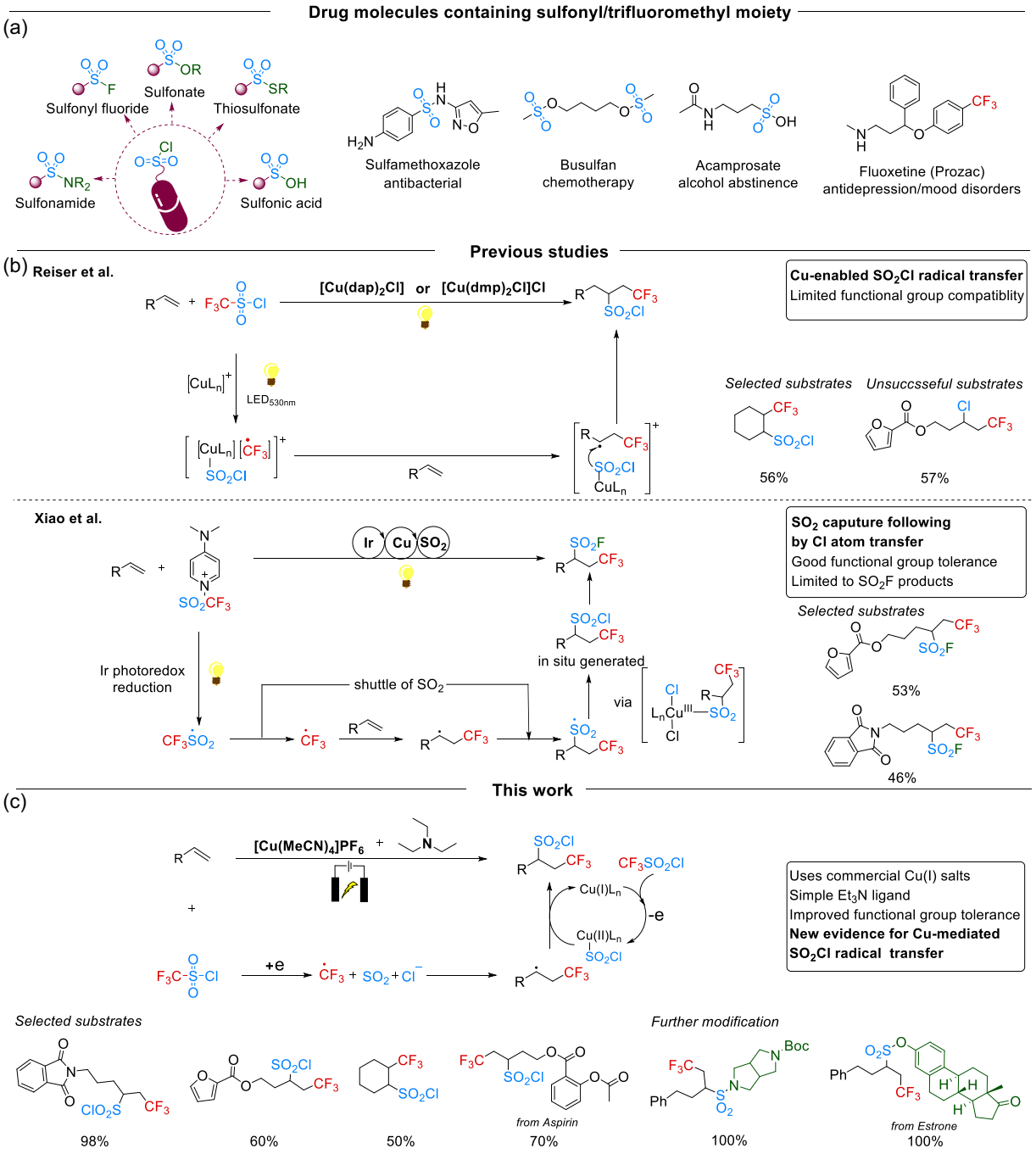

FIGURE 1 | (a) Synthetic versatility of the SO_2Cl moiety enabling access to diverse functional groups, along with representative drug molecules bearing sulfone (—SO_2—) and trifluoromethyl (—CF_3) motifs. (b) Previously reported photoredox-enabled alkene trifluoromethylchlorosulfonylation using Cu photocatalysis with 1,10-phenanthroline ligands. (c) Our electrochemical strategy for vicinal trifluoromethylchlorosulfonylation of alkenes using NEt_3 as a ligand and CF_3SO_2Cl as a bifunctional reagent.

intermediate. The CF_3 radical adds to the alkene, and the resulting carbon-centered radical is proposed to react directly with Cu-SO_2Cl to yield the difunctionalized product. In addition to its mechanistic novelty, this transformation enabled trifluoromethylchlorosulfonylation of a relatively broad array of alkene substrates. However, some limitations remained; for instance, the authors reported that certain Lewis basic groups (e.g., the furan derivative in Figure 1b) divert the reaction pathway toward trifluoromethylchlorination rather than the desired trifluoromethylchlorosulfonylation. Later, the same group also reported that Cu with 2,9-dimethyl-1,10-phenanthroline (dmp) ligand, a phenanthroline with different substituents from dap, could perform the same transformation as the $[Cu(dap)_2]Cl$ catalyst [28].

In a complementary approach, Xiao and coworkers[29] developed a dual Ir/Cu photoredox system using a bench-stable trifluoromethylsulfonyl pyridinium (TFSP) salt as a dual-source reagent for CF_3 and SO_2 (Figure 1b). Upon visible-light excitation, the Ir(III) catalyst undergoes oxidative quenching by TFSP to generate a trifluoromethylsulfonyl radical, which undergoes scission to

release a CF_3 radical. After alkene addition, the resulting alkyl radical undergoes in situ SO_2 reinsertion to form a persistent sulfonyl radical intermediate that is trapped by a chloride-ligated Cu(II) complex (with KCl as the chloride source), leading to a Cu(III) intermediate. Subsequent reductive elimination and fluoride–chloride exchange then yield the sulfonyl fluoride product. Meanwhile, single-electron transfer between Ir(IV) and Cu(I) regenerates the active catalytic species. This method showed good functional group tolerance and wide access to SO_2F-containing molecules. Although this method demonstrates the potential of TFSP in radical-mediated difunctionalization, it has several limitations. First, the SO_2Cl intermediate was not isolated or directly observed, and the reaction only furnished sulfonyl fluoride products. Second, the Cu catalytic cycle required suitable 1,10-phenanthroline ligands to promote efficient Cu catalysis.

Inspired by these literature reports as well as our own previous findings on trifluoromethylchlorination [29], we have developed a complementary Cu-catalyzed electrochemical trifluoromethyl chlorosulfonylation of alkenes using CF_3SO_2Cl as a bifunctional reagent (Figure 1c). Like photoredox catalysis, electrochemical methods allow precise control over redox events and facilitate paired redox processes; however, no photoexcitation of metal complexes is required under electrochemical conditions, which offers opportunities to broaden the ligand choice [30–38]. We envisioned that cathodic reduction could activate CF_3SO_2Cl to generate CF_3 radicals while simultaneously exploiting the redox flexibility of Cu(I)/Cu(II) at the anode to promote SO_2Cl transfer. We further hypothesized that without the need for photoactive Cu complexes, the Cu-SO_2Cl species might be better stabilized, leading to improved selectivity toward trifluoromethyl chlorosulfonylation for a wide scope of substrates.

Consistent with these proposals, we report herein that the use of commercially available $[Cu(MeCN)_4]PF_6$ in the presence of triethylamine (Et_3N) enables efficient and highly selective trifluoromethylchlorosulfonylation of alkenes. The reaction proceeds via electrochemical reduction of CF_3SO_2Cl, producing CF_3 radical and SO_2Cl^-. We propose that the CF_3 radical undergoes addition to the alkene, while the Cu catalyst traps SO_2Cl^- and then mediates transfer of the SO_2Cl moiety, likely via Cu(I)/Cu(II) anodic oxidation. This electrochemical system offers a broad substrate scope (for example, the furan derivative that was unsuccessful using Reiser's method furnished 60% yield of the desired product) and uses a simple and low-cost Et_3N ligand. Mechanistic studies provide experimental evidence, including isolation of the alkene chlorosulfonylation product, supporting SO_2Cl transfer from a Cu–SO_2Cl intermediate under these electrochemical conditions. Additionally, selected products could be further transformed into sulfonamides, sulfones, and other functionalized derivatives, highlighting the synthetic versatility of this platform.

2 | Results and Discussion

2.1 | Reaction Development

We initiated this study using 4-phenyl-1-butene (**1**) as a model substrate to develop an electrochemical trifluoromethyl chlorosulfonylation protocol (Table 1). The reaction was performed in MeCN with $LiClO_4$ as the supporting electrolyte, Et_3N as an additive, and $[Cu(MeCN)_4]PF_6$ as the Cu catalyst under constant voltage electrolysis (Figure S1). A voltage of 2.2 V was initially chosen based on the reduction peak potential of CF_3SO_2Cl ($E = -1.4$ V vs Ag/Ag^+) and oxidation peak potential of Cu(I) catalyst (E –0.9 V) as shown in Figure S2. To further validate these parameters, we measured the electrode potentials under the standard reaction conditions using a three-electrode setup with Ag/Ag^+ as the reference electrode. The anodic and cathodic potentials were determined to be +1.24 and −1.0 V, respectively (Figure S3), which are in reasonable agreement with potentials for CF_3SO_2Cl reduction and Cu(I) oxidation. Control experiments established the essential roles of both electricity and the Cu catalyst. No product formation was observed in the absence of electrolysis (entry 1). Similarly, in the absence of the Cu catalyst (entry 3), the reaction yielded **1a** (the chlorotrifluoromethylated product) in preference to **1b** (the trifluoromethylchlorosulfonylated product), with 5:1 selectivity. Lowering the Cu(I) catalyst loading to 1 mol% slowed the reaction (36% yield for **1b** and recovered **1**) but maintained the good selectivity toward **1b** over **1a** (6:1) (entry 13). This result highlights the crucial role of Cu in directing the reaction toward the target product **1b**. Furthermore, when $Cu(OTf)_2$ was used instead of $[Cu(MeCN)_4]PF_6$ (entry 7), both yield and selectivity dropped significantly (5% **1b**, 3:1 selectivity). This observation is consistent with our proposed mechanism in Figure 1c, in which Cu(I) undergoes anodic oxidation to Cu(II), which then participates in the delivery of SO_2Cl radicals. Upon applying a constant voltage of 2.2 V for 24 h, the desired trifluoromethylchlorosulfonylated product **1b** was obtained in 40% yield, along with 6% of the trifluoromethylchlorination side product **1a** (Table 1, entry 2). Interestingly, the omission of Et_3N completely shut down the reaction and led to full recovery of **1** (entry 4), underscoring its indispensable role, likely as both a sacrificial reductant [39, 40] and a weak binding ligand for Cu, which will be discussed in more detail in the mechanism section below [41]. Increasing the amount of Et_3N to 2 equiv (entry 5) improved the yield of **1b** to 57% while suppressing the formation of **1a** (1:9 selectivity). However, further increasing Et_3N to 3 equiv (entry 6) resulted in a decrease in both yield and selectivity.

Next, we varied the applied voltage. Increasing the potential from 2.2 to 2.5 V resulted in a significant increase in yield and selectivity, affording **1b** in 92% yield with a 1:15 selectivity over **1a** (entry 8). Further increases in voltage led to diminished performance: 3.0 V (entry 9) and 2.7 V (entry 10) both resulted in lower yields and poorer selectivity. We also evaluated the impact of ligand environment on Cu catalysis. When $[Cu(dap)_2]Cl$ was used instead of $[Cu(MeCN)_4]PF_6$ (entry 11), the reaction produced **1b** in good yield (72%), but with a significant increase in the formation of **1a** (27%, 1:3 selectivity). This result is consistent with strongly coordinating ligands, such as dap, altering the steric and electronic environment of the Cu center, thereby reducing the selectivity of the radical transfer step.

We also tested our chemistry using a commercial IKA ElectraSyn setup under either a constant voltage of 2.5 V or a constant current of 5 mA (entries 12 and 14). During the constant current experiment, the cell voltage gradually increased to 3.7 V over 24 h. In both cases, the reaction proceeded reproducibly;

TABLE 1 | Reaction Discovery and Development.

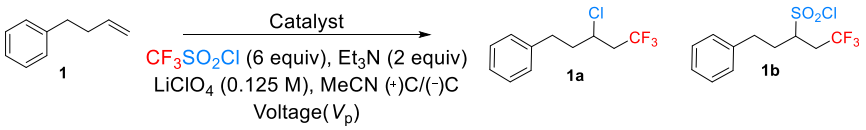

Entry	*Vp*	Et_3N (equiv)	Catalyst (mol%)	Time (h)	$[CF_3SO_2Cl]$ (equiv)	19F-NMR yield (%) (1a + 1b)	Selectivity (1a:1b)
1	N/A	1	$[(CH_3CN)_4Cu]PF_6$: 20	24	6	<1	N/A
2[a]	2.2	1	$[(CH_3CN)_4Cu]PF_6$: 20	24	6	06 + 40	1:7
3	2.2	1	N/A	24	6	51 + 11	5:1
4[a]	2.2	N/A	$[(CH_3CN)_4Cu]PF_6$: 20	24	6	02 + 02	1:1
5	2.2	2	$[(CH_3CN)_4Cu]PF_6$: 20	24	6	06 + 57	1:9
6	2.2	3	$[(CH_3CN)_4Cu]PF_6$: 20	24	6	07 + 41	1:7
7[a]	2.2	2	$Cu(OTf)_2$: 20	24	6	13 + 05	3:1
8	2.5	2	$[(CH_3CN)_4Cu]PF_6$: 20	24	6	06 + 92	1:15
9	3	2	$[(CH_3CN)_4Cu]PF_6$: 20	20	6	09 + 60	1:7
10	2.7	2	$[(CH_3CN)_4Cu]PF_6$: 20	24	6	08 + 85	1:11
11	2.5	2	$Cu(dap)_2Cl$: 1	24	6	27 + 72	1:3
12[b]	2.5	2	$[(CH_3CN)_4Cu]PF_6$: 20	24	6	21 + 72	1:3
13[a]	2.5	2	$[(CH_3CN)_4Cu]PF_6$: 1	24	6	06 + 36	1:6
14[b]	5 mA	2	$[(CH_3CN)_4Cu]PF_6$: 20	24	6	09 + 63	1:7

Reactions were performed under an argon atmosphere using 0.25 mmol of **1** (1 equiv) in 4 mL of acetonitrile. Yields were determined by ^{19}F NMR of the crude reaction mixture using hexafluorobenzene as an internal standard.
[a]Starting material recovered.
[b]ElectraSyn 2.0 was used.

however, the selectivity toward the desired chlorosulfonylated product **1b** was slightly lower than in our homebuilt cell. The measured faradaic efficiency is 17.8% under optimal conditions (Supporting Information).

Although the model substrate **1** afforded the sulfonyl chloride product **1b** in 92% ^{19}F NMR yield, the isolated yield was significantly lower (56%), due to the high reactivity of the sulfonyl chloride functional group. To facilitate product isolation and characterization, we in situ converted **1b** to the more stable sulfonamide derivative, **1c,** by adding benzylamine to the crude mixture after electrolysis [42]. This one-pot sequence yielded **1c** in a 48% isolated yield, which is comparable to the outcome from the reaction between isolated **1b** and benzyl amine (Figure S4). Throughout Figure 2, we report the ^{19}F NMR yields for sulfonyl chloride products ($-SO_2X$, X = Cl) and isolated yields for the corresponding sulfonamides ($-SO_2X$, X = NHBn).

To demonstrate the generality of this protocol, we evaluated a broad array of alkenes under the optimized conditions from Table 1. Figure 2 shows that a wide range of nonconjugated terminal alkenes are well tolerated. Allylbenzenes bearing a methoxy group or bromo group on the arene (**2b–4b**) gave high yields (98%, 72%, and 85%, respectively). 1-Allylnaphthalene, featuring an electron-rich aromatic system, also underwent efficient reaction, affording product **5b** in 60% yield. In all cases, the corresponding sulfonamide derivatives were isolated in moderate to good yields, ranging from 33% to 54%, following in situ derivatization (**2c–5c**).

Functionalized alkenes such as ether **6** also afforded a good yield (**6b**, 54%) with the corresponding sulfonamide **6c** isolated in 69% yield. Simple terminal alkenes, such as **7**, yielded the product **7b** in 98% yield, along with the corresponding sulfonamide **7c** in 44% yield. Alkyl ester- and bromo-groups (**8** and **9**) were also compatible, affording 92% and 62% yields, respectively. The sulfonamides **8c** and **9c** were isolated in yields of 56% and 50%. Substrates containing silyl groups also underwent smooth difunctionalization (**10b,** 66%). Notably, bisallylamine (**11**) and diethyl diallylmalonate (**12**) underwent cascade radical cyclization to yield five-membered ring products (**11b**, **12b**) in 72% and 70% yields, and corresponding sulfonamide **11c** and **12c** in 34% and 51% yields, respectively, confirming the radical nature of the reaction.

Next, we examined a series of aryl thioethers with varying electronic profiles (**13–17**), which are prone to overoxidation due to low onset oxidation potential ($E = 0.79–1.15$ V vs Ag/Ag^+) [29]. Indeed, sulfoxide byproducts were isolated for **16,** and no product was detected for **13** and **14** due to the oxidative decomposition under the optimized conditions (Figure S5). However, switching to alternating current (AC) electrolysis, which allows reversible oxidation and reduction of thioethers [29], mitigated this issue and restored product selectivity. Aryl thioethers with electron-donating (Me, iPr)

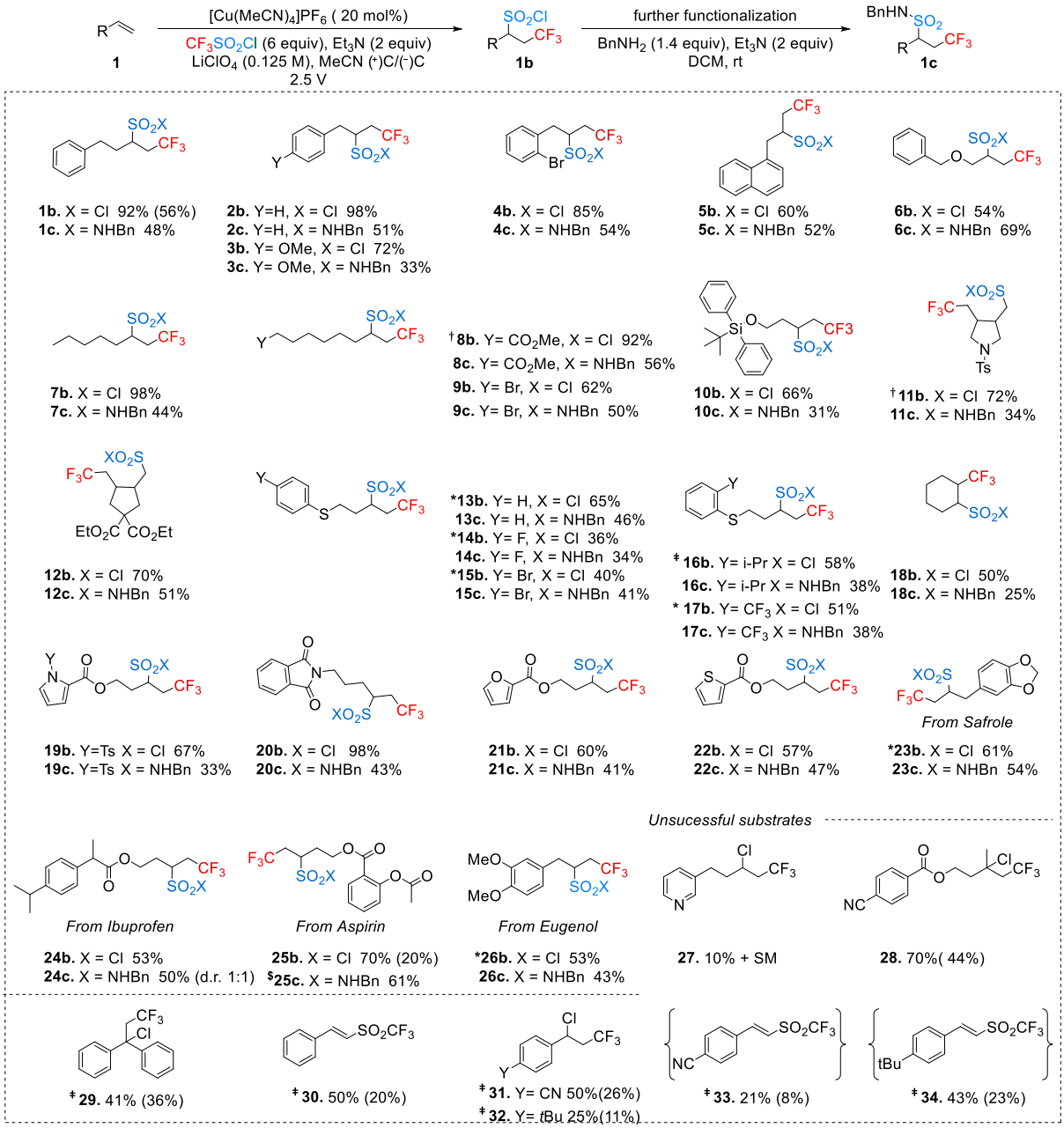

FIGURE 2 | Substrate scope for Cu-catalyzed electrochemical trifluoromethylchlorosulfonylation of alkenes. Reactions were performed on a 0.25 mmol scale. b. Yields were determined by ^{19}F NMR of the crude reaction mixture using hexafluorobenzene as an internal standard. The numbers in the parentheses are isolated yields. c. Isolated yields of the corresponding sulfonamide products are reported. *Reactions conducted under alternating current (AC) electrolysis conditions: 2.0 V, 10 Hz. †Reactions performed at 2.7 V. ‡Reactions performed at 2.0 V. $This product underwent hydrolysis and lost the acetyl group during the sulfonamidation step.

and electron-withdrawing substituents (F, Br, CF_3) at various positions afforded the corresponding sulfonyl chloride products (**13b–17b**) in moderate yields (36%–65%).

Furthermore, cyclic alkenes such as **18** afford products **18b** and **18c** in 50% and 25% yield, respectively. **18c** was isolated as a single diastereomer, in contrast to the previously reported photocatalytic reaction, which produced a diastereomeric mixture in a 3:2 ratio [27]. Heteroarene-containing alkenes such as tosyl-protected pyrrole (**19**), furan and thiophene derivatives (**21**, **22**) proceeded smoothly (**19b** 67%, **21b** 60%, and **22b** 57% respectively), while phthalimide (**20**) delivered the product (**20b**) in an excellent yield of 98%. The corresponding sulfonamide derivatives **19c–22c** were isolated in moderate to good yield (–33%–47%). Note that some of these compounds were not tolerated by the previous photocatalytic protocol (Figure S6).

Finally, we applied our protocol to drug-derived alkenes **23–26**. All substrates underwent smooth trifluoromethyl chlorosulfonylation, affording the difunctionalized products **23b–26b** in yields of 53%–70%. Subsequent sulfonamide derivatization also proceeded efficiently, delivering the corresponding products in –50% isolated yields, except **25c**, which lost an acetyl group due to hydrolysis during the sulfonamidation step.

There were a few unsuccessful substrates. For example, pyridine-derived alkene **27** failed to undergo the desired reaction, possibly due to its coordination to the Cu ions [43, 44] or the formation of an electrochemically inactive pyridinium adduct with CF_3SO_2Cl [45]. 1,1-Disubstituted alkenes selectively afforded chlorotrifluoromethylated product **28**. In addition, styrene derivatives failed to undergo clean difunctionalization, instead yielding mixtures of chlorotrifluoromethylated products (**29, 31,** and **32**) and trifluoromethylsulfonated products (**30, 33,** and **34**). The observed divergence likely originates from the increased stability of benzylic radical intermediates formed after the initial radical addition of either CF_3• or CF_3SO_2•. These intermediates can undergo chlorine atom transfer to yield either chlorotrifluoromethylation or chlorotrifluorosulfonation products. Notably, the latter may also undergo β-elimination, driven by the acidic α-proton adjacent to the sulfonyl group, leading to the formation of conjugated vinyl triflates. The π-system of styrenes may also disfavor efficient SO_2Cl transfer, thereby contributing to the diminished selectivity and divergence in product outcomes. We also found that styrene derivatives were prone to over-oxidation at 2.5 V, leading to substrate decomposition. To mitigate this issue, the reactions were conducted at a lower potential (2.0 V), which improved substrate stability but maintained the divergent product distribution. These observations are in line with literature reports [28, 45, 46], which describe similar Cu-catalyzed chlorotrifluoromethylation and vinyl triflate formation from styrene derivatives.

Sulfonyl chlorides have long served as versatile electrophiles in organic synthesis [25, 47], as they undergo rapid and selective coupling with a wide variety of nucleophiles. To showcase the synthetic utility and diversification potential of the trifluoromethylchlorosulfonylated products, we subjected the isolated compound **1b** to a series of nucleophiles (Figure 3). These transformations proceeded efficiently, affording structurally diverse sulfonamide (**1c–1h**), sulfonate (**1i–1j**), thiosulfonate (**1k**), and sulfonyl fluoride (**1l**) products in good to excellent yields. Notably, medicinally relevant amines, including derivatives from paroxetine and estrone, reacted to afford **1h** and **1j** in 86% and 84% isolated yield, respectively, further demonstrating the applicability of this protocol for late-stage functionalization. Together, these results highlight the broad nucleophile compatibility and downstream utility of the electrochemically generated trifluoromethylchlorosulfonylated products, providing access to a wide array of sulfone-containing motifs from a single, operationally simple starting point.

2.2 | Mechanistic Study

To interrogate the underlying mechanism of the electrochemical trifluoromethylchlorosulfonylation, we considered two plausible pathways based on literature precedents (Figure 4a). In Pathway 1, CF_3SO_2Cl undergoes cathodic reduction to generate CF_3• along with SO_2 and Cl^-. The CF_3• adds to the alkene, forming a carbon-centered radical intermediate, which then undergoes SO_2 insertion to afford a sulfonyl radical. Subsequent chlorine atom transfer from a Cu(II)–Cl species, generated at the anode, delivers the final product. Pathway 2 also begins with the electrogeneration of CF_3•, which then adds to the alkene. However, instead of SO_2 shuttling through the solution, Cu(I) reacts with CF_3SO_2Cl to generate a Cu(II)–SO_2Cl species, which then transfers SO_2Cl to the alkyl radical, resulting in the formation of the final difunctionalization product. This mechanism is consistent with Reiser's recent proposal of Cu-mediated SO_2Cl transfer [27].

To probe the operative mechanism, we performed a series of control experiments as follows. First, 10 equiv of 2,2,6,6-tetramethylpiperidinyloxy (TEMPO) was added as a radical scavenger. Under the standard conditions, this resulted in the complete suppression of the desired reaction and 65% TEMPO-CF_3 adduct (Figure 4b and S7). This result is consistent with the generation of CF_3 radicals being the initiation step shared by both pathways. Under the standard reaction conditions, the formation of SO_2 gas was confirmed via the decolorization of permanganate stain (Figure S8). To probe the relevance of SO_2 shuttling in the reaction, we tested the effect of adding additional SO_2 to

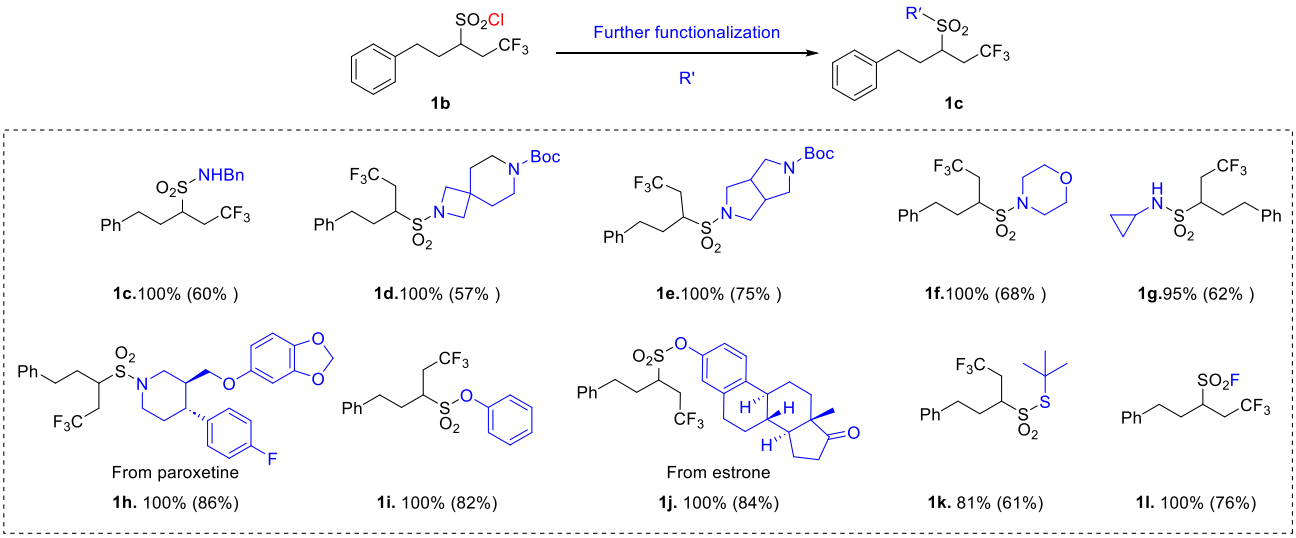

FIGURE 3 | Late-stage functionalization and synthetic utility of trifluoromethylchlorosulfonylated products. Reactions were performed on a 0.125 mmol scale. Yields were determined by ^{19}F NMR analysis of the crude reaction mixture using hexafluorobenzene as the internal standard. Isolated yields are shown in parentheses.

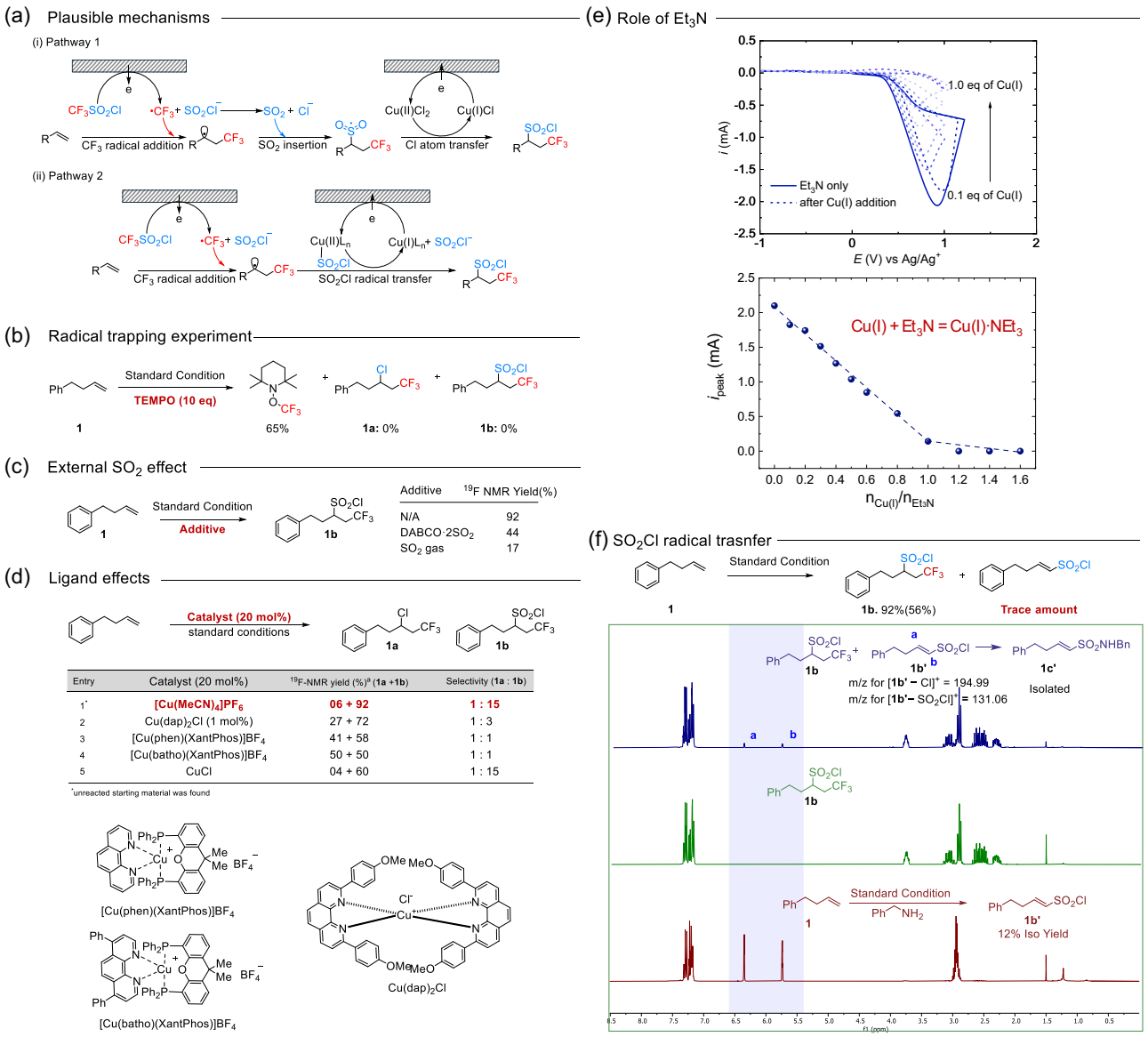

FIGURE 4 | (a) Proposed mechanistic pathways: Pathway 1 involves CF_3 radical addition followed by SO_2 insertion and Cu(II)-mediated Cl transfer; Pathway 2 involves Cu-mediated SO_2Cl radical transfer. (b) Radical trapping experiment using TEMPO. (c) Control experiments with external SO_2 sources. (d) Control experiments with different ligands. (e) Electrochemical titration of Et_3N using $[Cu(MeCN)_4]PF_6$: (top) Cyclic voltammograms of 0.25 mmol Et_3N in 4 mL MeCN after adding 0.1–1 equiv of $[Cu(MeCN)_4]PF_6$. The anodic waves at –1 V correspond to the oxidation of free Et_3N. (bottom) A plot of the anodic peak currents at –1 V versus the molar ratio of $[Cu(MeCN)_4]PF_6$ and Et_3N ($n_{Cu(I)}/n_{Et3N}$). Experiments were conducted in 0.125 M $LiClO_4$/MeCN using a glassy carbon working electrode at a scan rate of 1 V/s. (f) ^1H NMR and mass spectrometric evidence for chlorosulfonylation side product (**1b′**): blue trace shows the ^1H NMR spectrum for a mixture of **1b** and **1b′** isolated from the reaction mixture; green and red traces are isolated spectra of pure **1b** and **1b′**, respectively. All yields reported were determined by ^{19}F NMR using hexafluorobenzene as an internal standard; isolated yields are reported where noted.

the reaction mixture, either as gaseous SO_2 (g) or as bench-stable DABCO·2SO_2 (Figure 4c). Both additives led to significantly reduced product yields, showing that higher concentrations of free SO_2 inhibit product formation. This observation suggests against Pathway 1.

Given the known ligand sensitivity in Cu-mediated radical transfer reactions [27, 28, 48], we next examined the effect of ligands on the efficiency and selectivity of our electrochemical protocol (Figure 4d). Strongly coordinating ligands such as Xantphos [49] and bathophenanthroline [25] significantly eroded the **1a**:**1b** selectivity, despite high mass balance (entries 3,4). The sterically hindered dap ligand shows improved selectivity toward **1b** (entry 2), while simple Cu salts, such as CuCl, provided high selectivity toward **1b** (entry 5). The adverse effect of the strong, saturated coordination environment around Cu on reaction selectivity is consistent with the proposed Cu-mediated SO_2Cl group transfer mechanism in Pathway 2.

The finding above led us to consider a possible role of Et_3N as a weak ligand for Cu(I). To investigate the coordination chemistry between Et_3N and $[Cu(MeCN)_4]PF_6$, we performed an electrochemical titration experiment. Progressive addition of $[Cu(MeCN)_4]PF_6$ resulted in a marked decrease in the Et_3N

oxidation peak at −1.0 V, which disappeared entirely after the addition of one equivalent of $[Cu(MeCN)_4]PF_6$ (Figure 4e). This result suggests that Et_3N and Cu(I) undergo a 1:1 stoichiometric reaction to form a Cu(I)–Et_3N complex [41], which retains coordination sites for SO_2Cl to bind the Cu center and subsequently participate in SO_2Cl group transfer.

Additional evidence supporting Pathway 2 was obtained through mass spectrometric analysis (Figure S9) and ^1H NMR characterization of the product mixture (Figure 4f). Alongside the signal from the desired product **1b**, two additional mass signals at $m/z = 194.99$ and 131.06 were detected by gas chromatography–mass spectrometry (GC–MS), corresponding to two fragments from the chlorosulfonylation product of **1** (i.e., $[\mathbf{1b}'-Cl]^+$ and $[\mathbf{1b}'-SO_2Cl]^+$). Additionally, a pair of characteristic vinyl proton peaks at δ 6.38 (d, $J = 1.9$ Hz, 1H) and 5.77 (q, $J = 1.5$ Hz, 1H) [50] was observed in the ^1H NMR spectrum of an aliquot collected during chromatographic separation of the reaction mixture, further suggesting the presence of **1b′** as a minor byproduct.

Although isolating **1b′** proved challenging, post-reaction derivatization with benzylamine enabled the isolation and confirmation of its sulfonamidation product **1f**, albeit in a low yield (<4%). Interestingly, the addition of benzylamine to the reaction unexpectedly promoted the chlorosulfonylation pathway, yielding isolable **1b′** (its ^1H NMR spectrum is provided in the bottom panel of Figure 4f). Comparison of the ^1H NMR spectra confirmed the chlorosulfonylation product identity. The presence of the sulfonylchlorinated product **1b′** is evidence that the SO_2Cl moiety is transferred intact as a radical via a Cu–SO_2Cl species during the reaction, with the amine ligand playing a critical role. The Cu–SO_2Cl species could be formed via the reaction of Cu(I), Et_3N, and CF_3SO_2Cl. Mixing these components led to the appearance of a Cu–CF_3 signal near −28 ppm [51, 52] in the ^{19}F NMR spectrum (Figures S10–S13). Based on mass balance considerations, the concomitant formation of a Cu–SO_2Cl species under these conditions is likely. However, we have not yet obtained direct evidence for its presence.

Taken together, these mechanistic studies support Pathway 2, which involves the addition of a CF_3 radical to an alkene followed by Cu-mediated transfer of an SO_2Cl radical, facilitated by weakly bound amine ligands. We also note that, in the absence of copper, partial selectivity for **1b** was still observed (Table 1, Entry 3); a likely noncatalyzed pathway accounting for this outcome is discussed in Figure S14.

3 | Conclusions

In conclusion, this report describes the development of a selective electrochemical trifluoromethylchlorosulfonylation of unactivated alkenes using CF_3SO_2Cl and Cu catalysis. This method uses a simple Et_3N ligand and leverages the redox activity of Cu(I)/Cu(II) to mediate SO_2Cl transfer, a mechanistic feature consistent with Reiser's previous work and our own control experiments, including analysis of the key chlorosulfonylation side products. The broad substrate scope, encompassing alkyl, aryl, heteroaryl, and functionalized alkenes, underscores the transformation's versatility. Moreover, the resultant sulfonyl chlorides serve as valuable intermediates for downstream derivatization into a variety of sulfone-containing motifs of medicinal relevance. Overall, this work establishes a synthetically practical electrochemical strategy that is complementary to the previous photocatalytic methods for the difunctionalization of alkenes and also opens new avenues for electrosynthesizing the sulfonylated compounds via Cu-mediated SO_2Cl transfer.

4 | Materials and Methods

4.1 | General Information

All chemicals and reagents were obtained from commercial vendors and used without further purification. The CF_3SO_2Cl reagent was stored in a glove box freezer at −20°C, and fresh aliquots were removed from the glove box and added immediately to the reaction. All reactions were carried out in oven-dried glassware under a positive pressure of argon using Schlenk line techniques. Analytical thin-layer chromatography (TLC) was routinely used to monitor the progress of the reactions. TLC was performed using precoated glass plates with 230–400 mesh silica gel impregnated with a fluorescent indicator (250 nm). Visualization was accomplished using UV light, potassium permanganate. Flash chromatography was performed on silica gel flash chromatography columns, Teledyne Isco Combi Flash Rf system utilizing normal phase precolumn cartridges and gold high-performance columns. All proton nuclear magnetic resonance (^1H NMR) spectra, all carbon nuclear magnetic resonance (^{13}C NMR) spectra, and all fluorine nuclear magnetic resonance (^{19}F NMR) spectra were recorded with Agilent MR-400 MHz or Bruker Avance NEO 500 MHz or Bruker Avance NEO 300 MHz spectrometers. Chemical shifts were expressed in parts per million (δ scale) and were referenced to residual $CHCl_3$ (^1H: δ 7.26 ppm, ^{13}C: δ 77.16 ppm) and C_6F_6 (^{19}F: δ-163 ppm). NMR data are presented as follows: chemical shift (δ), multiplicity (s = singlet, d = doublet, t = triplet, q = quartet, m = multiplet, dd = doublet of doublet), coupling constants in Hz, and integration. Crude ^{19}F NMR yields of all trifluoromethylated compounds were determined using hexafluorobenzene (PhF_6) as an internal standard. High-resolution mass spectra were recorded on either a Thermo Scientific Explories 120 Orbitrap mass spectrometer or an Agilent 7200 GC–MS QTOF mass spectrometer. GC–MS analyses were conducted on an Agilent 8890 GC System with 5977 B GC/MSD equipped with a HP-5MScapillary column (30 m length, 0.28 mm id, and 0.25 μm film thickness). All AC experiments were conducted using a function generator (Agilent 33210A) in conjunction with a modulated power supply (ACCEL Instruments TS200-0A). Glassy carbon (vitreous) plates (100 × 100 mm) were purchased from SPI Supplies. DC experiments were carried out using an IKA ElectraSyn 2.0. The discharge voltage, frequency, and waveform were monitored using an oscilloscope (SIGLENT Technologies SDS1202X-E). Voltammetry experiments were carried out using a CHI 650E potentiostat.

4.1.1 | General Procedure for Trifluoromethylchloro-Sulfonylation of Alkenes via DC and AC Electrolysis

In an oven-dried 10 mL conical Schlenk flask equipped with a triangular magnetic stir bar, $LiClO_4$ (53 mg, 0.5 mmol, 2.0 equiv),

$[Cu(MeCN)_4]PF_6$ (18 mg, 20 mol%), Et_3N (70 µL, 0.5 mmol, 2.0 equiv), the olefin substrate (0.25 mmol, 1.0 equiv), and anhydrous acetonitrile (4 mL) were added under an argon atmosphere. CF_3SO_2Cl (160 µL, 1.5 mmol, 6.0 equiv) was then introduced to the reaction mixture. Two carbon plate electrodes (3 mm in thickness, 1 cm in width, and ~10 cm in length) were then inserted into the reaction flask with an electrode–electrode separation of ~1 mm and immersed ~2 cm into the solution. The electrodes were connected to a waveform generator and amplifier (see Figure S1). Electrolysis was conducted under one of the following conditions: constant voltage (2.0, 2.5, or 2.7 V), or AC square wave (amplitude = 2.0 V, frequency = 10 Hz), depending on the substrate. The mixture was stirred at room temperature under electrochemical conditions until full consumption of the olefin substrate was confirmed by TLC. Electrodes were then removed, and hexafluorobenzene (15 µL, 0.125 mmol, 0.5 equiv) was added as an internal standard. After 2 min of stirring, an aliquot was taken for crude ^{19}F NMR analysis. The reaction mixture was diluted with deionized water (5 mL) and extracted with DCM (3 × 15 mL). The combined organic extracts were washed with saturated NaCl solution, dried over Na_2SO_4, and concentrated under reduced pressure. The crude residue was purified by gradient flash chromatography on silica gel to yield the desired product.

4.1.2 | Substrate Synthesis, Further Functionalization, and Control Experiments

Detailed information regarding these methods can be found in the Supporting Information.

Author Contributions

The manuscript was written through the contributions of all authors.

Acknowledgments

This work was supported by the NSF Center for Synthetic Organic Electrochemistry, CHE-2002158 and 2503773, the University of Utah, and the Alfred P. Sloan Foundation (Grant # FH-2023–20829). ChatGPT was used to improve the language and clarity of the manuscript during its preparation.

Conflicts of Interest

The authors declare no conflicts of interest.

Data Availability Statement

The data that support the findings of this study are available in the supplementary material of this article.

References

1. J. Clayden, N. Greeves, and S. Warren, Organic Chemistry (Oxford University Press, 2012), ISBN 0199270295.

2. L. Surhone, M. Tennoe, and S. Henssonow, Vicinal Difunctionalization (Betascript Publishing, 2010).

3. R.-J. Song, Y. Liu, Y.-X. Xie, and J.-H. Li, "Difunctionalization of Acrylamides through C–H Oxidative Radical Coupling: New Approaches to Oxindoles," *Synthesis* 47 (2015): 1195–1209.

4. J.-R. Chen, X.-Y. Yu, and W.-J. Xiao, "Tandem Radical Cyclization of N-Arylacrylamides: An Emerging Platform for the Construction of 3, 3-disubstituted oxindoles," *Synthesis* 47 (2015): 604–629.

5. G. Yin, X. Mu, and G. Liu, "Palladium (II)-Catalyzed Oxidative Difunctionalization of Alkenes: Bond Forming at a High-Valent Palladium Center," *Accounts of Chemical Research* 49 (2016): 2413–2423.

6. R. Giri and S. Kc, "Strategies toward Dicarbofunctionalization of Unactivated Olefins by Combined Heck Carbometalation and Cross-Coupling," *The Journal of Organic Chemistry* 83 (2018): 3013–3022.

7. R. K. Dhungana, S. Kc, P. Basnet, and R. Giri, "Transition Metal-Catalyzed Dicarbofunctionalization of Unactivated Olefins," *Chemical Record* 18 (2018): 1314–1340.

8. J. Lin, R. J. Song, M. Hu, and J. H. Li, "Recent Advances in the Intermolecular Oxidative Difunctionalization of Alkenes," *Chemical Record* 19 (2019): 440–451.

9. Y. C. Wu, Y. T. Xiao, Y. Z. Yang, R. J. Song, and J. H. Li, "Recent Advances in Silver-Mediated Radical Difunctionalization of Alkenes," *ChemCatChem* 12 (2020): 5312–5329.

10. Z.-L. Li, G.-C. Fang, Q.-S. Gu, and X.-Y. Liu, "Recent Advances in Copper-Catalysed Radical-Involved Asymmetric 1,2-Difunctionalization of Alkenes," *Chemical Society Reviews* 49 (2020): 32–48, https://doi.org/10.1039/C9CS00681H.

11. Y. Wang, Y. Bao, M. Tang, Z. Ye, Z. Yuan, and G. Zhu, "Recent Advances in Difunctionalization of Alkenes Using Pyridinium Salts as Radical Precursors," *Chemical Communications* 58 (2022): 3847–3864.

12. J. Sun, L. Wang, G. Zheng, and Q. Zhang, "Recent Advances in Three-Component Radical Acylative Difunctionalization of Unsaturated Carbon–carbon Bonds," *Organic Chemistry Frontiers* 10 (2023): 4488–4515.

13. Z.-L. Zhou, Y. Zhang, P.-Z. Cui, and J.-H. Li, "Photo-/Electrocatalytic Difunctionalization of Alkenes Enabled by C–H Radical Functionalization," *Chemistry – A European Journal* 30 (2024): e202402458, https://doi.org/10.1002/chem.202402458.

14. H. L. Yale, "The Trifluoromethyl Group in Medical Chemistry," *Journal of Medicinal Chemistry* 1 (1958): 121–133.

15. A. Studer, "A "Renaissance" in Radical Trifluoromethylation," *Angewandte Chemie International Edition* 51 (2012): 8950–8958, https://doi.org/10.1002/anie.201202624.

16. W. K. Hagmann, "The Many Roles for Fluorine in Medicinal Chemistry," *Journal of Medicinal Chemistry* 51 (2008): 4359–4369, https://doi.org/10.1021/jm800219f.

17. O. A. Tomashenko and V. V. Grushin, "Aromatic Trifluoromethylation with Metal Complexes," *Chemical Reviews* 111 (2011): 4475–4521, https://doi.org/10.1021/cr1004293.

18. K. Hofman, N.-W. Liu, and G. Manolikakes, "Radicals and Sulfur Dioxide: A Versatile Combination for the Construction of Sulfonyl-Containing Molecules," *Chemistry – A European Journal* 24 (2018): 11852–11863, https://doi.org/10.1002/chem.201705470.

19. Y.-J. Zhang, M.-L. Li, H.-X. Hu, and F. Teng, "Recent Advances in Palladium-Catalyzed Sulfonylation via SO2 Insertion," *Organic & Biomolecular Chemistry* 22 (2024): 5868–5885, https://doi.org/10.1039/D4OB00667D.

20. M. Feng, B. Tang, S. H. Liang, and X. Jiang, "Sulfur Containing Scaffolds in Drugs: Synthesis and Application in Medicinal Chemistry," *Current Topics in Medicinal Chemistry* 16 (2016): 1200–1216.

21. E. J. Emmett and M. C. Willis, "The Development and Application of Sulfur Dioxide Surrogates in Synthetic Organic Chemistry," *Asian Journal of Organic Chemistry* 4 (2015): 602–611, https://doi.org/10.1002/ajoc.201500103.

22. B. M. Trost and C. A. Kalnmals, "Sulfones as Chemical Chameleons: Versatile Synthetic Equivalents of Small-Molecule Synthons," *Chemistry–A European Journal* 25 (2019): 11193–11213.

23. G. Chen and Z. Lian, "Multicomponent Reactions Based on SO2 Surrogates: Recent Advances," *European Journal of Organic Chemistry* 26 (2023): e202300217, https://doi.org/10.1002/ejoc.202300217.

24. J. J. Garrido-González, K. Medrano-Uribe, C. Rosso, J. Humbrías-Martín, and L. Dell'Amico, "Photocatalytic Synthesis and Functionalization of Sulfones, Sulfonamides and Sulfoximines," *Chemistry – A European Journal* 30 (2024): e202401307, https://doi.org/10.1002/chem.202401307.

25. O. S. Liashuk, V. A. Andriashvili, A. O. Tolmachev, and O. O. Grygorenko, "Chemoselective Reactions of Functionalized Sulfonyl Halides," *Chemical Record* 24 (2024): e202300256, https://doi.org/10.1002/tcr.202300256.

26. H. Guyon, H. Chachignon, and D. Cahard, "CF3SO2X (X = Na, Cl) as Reagents for Trifluoromethylation, Trifluoromethylsulfenyl-, -Sulfinyl- and -Sulfonylation. Part 1: Use of CF3SO2Na," *Beilstein Journal of Organic Chemistry* 13 (2017): 2764–2799, https://doi.org/10.3762/bjoc.13.272.

27. D. B. Bagal, G. Kachkovskyi, M. Knorn, T. Rawner, B. M. Bhanage, and O. Reiser, "Trifluoromethylchlorosulfonylation of Alkenes: Evidence for an Inner-Sphere Mechanism by a Copper Phenanthroline Photoredox Catalyst," *Angewandte Chemie International Edition, in English* 54 (2015): 6999–7002, https://doi.org/10.1002/anie.201501880.

28. S. Engl and O. Reiser, "Making Copper Photocatalysis Even More Robust and Economic: Photoredox Catalysis with [CuII(dmp)2Cl]Cl," *European Journal of Organic Chemistry* 2020 (2020): 1523–1533, https://doi.org/10.1002/ejoc.201900839.

29. S. Rodrigo, A. Hazra, J. P. Mahajan, H. M. Nguyen, and L. Luo, "Overcoming the Potential Window-Limited Functional Group Compatibility by Alternating Current Electrolysis," *Journal of the American Chemical Society* 145 (2023): 21851–21859, https://doi.org/10.1021/jacs.3c05802.

30. N. E. S. Tay, D. Lehnherr, and T. Rovis, "Photons or Electrons? A Critical Comparison of Electrochemistry and Photoredox Catalysis for Organic Synthesis," *Chemical Reviews* 122 (2022): 2487–2649, https://doi.org/10.1021/acs.chemrev.1c00384.

31. R. H. Verschueren and W. M. De Borggraeve, "Electrochemistry and Photoredox Catalysis: A Comparative Evaluation in Organic Synthesis," *Molecules* 24 (2019): 2122, 10.3390/molecules24112122PubMed.

32. C. P. Chernowsky, A. F. Chmiel, and Z. K. Wickens, "Electrochemical Activation of Diverse Conventional Photoredox Catalysts Induces Potent Photoreductant Activity," *Angewandte Chemie International Edition, in English* 60 (2021): 21418–21425.

33. M. Lepori, S. Schmid, and J. P. Barham, "Photoredox Catalysis Harvesting Multiple Photon or Electrochemical Energies," *Beilstein Journal of Organic Chemistry* 19 (2023): 1055–1145.

34. J. Quintaine, L. Saudan, F. Santoro, G. Oddon, E. Labbé, and O. Buriez, "Monitoring and Assessing Iridium-Promoted Photoredox Catalysis by Electrochemistry," *ACS Catalysis* 13 (2023): 14894–14906.

35. J. Liu, L. Lu, D. Wood, and S. Lin, "New Redox Strategies in Organic Synthesis by Means of Electrochemistry and Photochemistry," *ACS Central Science* 6 (2020): 1317–1340, https://doi.org/10.1021/acscentsci.0c00549.

36. N. L. Reed and T. P. Yoon, "Oxidase Reactions in Photoredox Catalysis," *Chemical Society Reviews* 50 (2021): 2954–2967.

37. C. Y. Sun, T. J. Lin, Y. Y. Chen, H. L. Li, and C. W. Chiang, "Synergistic Photoredox and Electrochemical Catalysis in Organic Synthesis and Late-Stage Functionalizations," *ChemCatChem* 16 (2024): e202301537.

38. N. A. Romero and D. A. Nicewicz, "Organic Photoredox Catalysis," *Chemical Reviews* 116 (2016): 10075–10166, https://doi.org/10.1021/acs.chemrev.6b00057.

39. S. R. Reddy, S. Bhulakshmi, T. M. Chacko, et al., "Triethylamine-Mediated Synthesis of Bioactive Heterocycles," in Organic Synthesis, Natural Products Isolation, Drug Design, Industry and the Environment, (Eds: C. Mukhopadhyay, B. Banerjee, D. Gruyter Brill) (2023).

40. W. Jud, S. Maljuric, C. O. Kappe, and D. Cantillo, "Cathodic C–H Trifluoromethylation of Arenes and Heteroarenes Enabled by an in Situ-Generated Triflyltriethylammonium Complex," *Organic Letters* 21 (2019): 7970–7975, https://doi.org/10.1021/acs.orglett.9b02948.

41. J. T. Yoke III, J. F. Weiss, and G. Tollin, "Reactions of Triethylamine with Copper (I) and Copper (II) Halides," *Inorganic Chemistry* 2 (1963): 1210–1216.

42. F. Carta, S. Andrea, and C. T. Supuran, "Sulfonamides: A Patent Review (2008 – 2012," *Expert Opinion on Therapeutic Patents* 22 (2012): 747–758, https://doi.org/10.1517/13543776.2012.698264.

43. Z. Liu, M. F. Qayyum, C. Wu, et al., "A Codeposition Route to CuI–Pyridine Coordination Complexes for Organic Light-Emitting Diodes," *Journal of the American Chemical Society* 133 (2011): 3700–3703, https://doi.org/10.1021/ja1065653.

44. M. Malik, A. Świtlicka, A. Bieńko, et al., "Copper(ii) Complexes with 2-Ethylpyridine and Related Hydroxyl Pyridine Derivatives: Structural, Spectroscopic, Magnetic and Anticancer in Vitro Studies," *RSC Advances* 12 (2022): 27648–27665, https://doi.org/10.1039/D2RA05133H.

45. W. Zhang, J.-H. Lin, and J.-C. Xiao, "Cu-Catalyzed Chlorotrifluoromethylation of Alkenes with CF3SO2Cl," *Journal of Fluorine Chemistry* 215 (2018): 25–31, https://doi.org/10.1016/j.jfluchem.2018.09.001.

46. M. Alkan-Zambada and X. Cu Hu, "Photoredox Catalysts Supported by a 4,6-Disubstituted 2,2′-Bipyridine Ligand: Application in Chlorotrifluoromethylation of Alkenes," *Organometallics* 37 (2018): 3928–3935, https://doi.org/10.1021/acs.organomet.8b00585.

47. T. Rawner, M. Knorn, E. Lutsker, A. Hossain, and O. Reiser, "Synthesis of Trifluoromethylated Sultones from Alkenols Using a Copper Photoredox Catalyst," *The Journal of Organic Chemistry* 81 (2016): 7139–7147, https://doi.org/10.1021/acs.joc.6b01001.

48. Y.-F. Yang, F. Xiao, J.-H. Lin, and J.-C. Xiao, "The Shuttle of Sulfur Dioxide: Iridium/Copper-Cocatalyzed Trifluoromethylfluorosulfonylation of Alkenes," *Advanced Synthesis & Catalysis* 365 (2023): 301–306, https://doi.org/10.1002/adsc.202201286.

49. M. Viciano-Chumillas, J. M. Carbonell-Vilar, D. Armentano, and J. Cano, "Influence of Xantphos Derivative Ligands on the Coordination in Their Copper(I) and Silver(I) Complexes," *European Journal of Inorganic Chemistry* 2019 (2019): 2982–2989, https://doi.org/10.1002/ejic.201900323.

50. B. B. Metaferia, B. J. Fetterolf, S. Shazad-ul-Hussan, et al., "Synthesis of Natural Product-Inspired Inhibitors of Mycobacterium Tuberculosis Mycothiol-Associated Enzymes: The First Inhibitors of GlcNAc-Ins Deacetylase," *Journal of Medicinal Chemistry* 50 (2007): 6326–6336, https://doi.org/10.1021/jm070669h.

51. T. Rühl, W. Rafique, V. T. Lien, and P. J. Riss, "Cu(i)-Mediated 18F-Trifluoromethylation of Arenes: Rapid Synthesis of 18F-Labeled Trifluoromethyl Arenes," *Chemical Communications* 50 (2014): 6056–6059, https://doi.org/10.1039/C4CC01641F.

52. H. Morimoto, T. Tsubogo, N. D. Litvinas, and J. F. Hartwig, "A Broadly Applicable Copper Reagent for Trifluoromethylations and Perfluoroalkylations of Aryl Iodides and Bromides," *Angewandte Chemie International Edition, in English* 50 (2011): 3793–3798, https://doi.org/10.1002/anie.201100633.

Supporting Information

Additional supporting information can be found online in the Supporting Information section. **Supporting Fig. 1:** Visualization of the variables

present in Equations S1-3. **Supporting Fig. 2:** The *Design x,y* column is set as shown (highlighted by the green box). **Supporting Fig. 3:** Positioning the crosshair (+) over two markers to obtain their coordinates. a) Positioning the crosshair on the first alignment marker (*M0*) and b) on the second alignment marker (*M1*). **Supporting Fig. 4:** Schematic drawing of the print cell used when printing with the hydrogels. Two pieces of single-sided tape act as spacers for confining the hydrogel photoresist. **Supporting Fig. 5:** Schematic of the alignment accuracy calculation. a) Multi-point tool (green) and elliptical tool (red) from ImageJ. b) Center of the alignment marker identification. c) Coordinates corresponding to the four alignment marker centers (selected points, +) and calculated center of the square (dot). d) Second print center circle (red dot) coordinates. **Supporting Table1:** Descriptions of variables present in equations S1-3 along with their units. **Supporting Table 2:** Composition of the acrylic acid-based hydrogel photoresist. **Supporting Table 3:** Composition of the phenylboronic acid-based hydrogel photoresist.